

Return of Deep Space in Weilheim Ground Station

**Marcin Gnat^{a*}, Martin Häusler^b, Markus Limbach^c, Klaus Schlickenrieder^d, Erica Barkasz^e,
Amanuel Geda^f, Christian Oetl^g**

^a *Communications and Ground Stations, German Space Operations Center, German Aerospace Center (DLR), Muenchenerstrasse 20, 82234 Wessling, Germany, marcin.gnat@dlr.de*

^b *Communications and Ground Stations, German Space Operations Center, German Aerospace Center (DLR), Reichenbergstrasse 8, 82362 Weilheim, Germany, martin.haeusler@dlr.de*

^c *SAR Technology, Microwaves and Radar Institute, German Aerospace Center (DLR), Muenchenerstrasse 20, 82234 Wessling, Germany, markus.limbach@dlr.de*

^d *Communications and Ground Stations, German Space Operations Center, German Aerospace Center (DLR), Reichenbergstrasse 8, 82362 Weilheim, Germany, klaus.schlickenrieder@dlr.de*

^e *Communications and Ground Stations, German Space Operations Center, German Aerospace Center (DLR), Reichenbergstrasse 8, 82362 Weilheim, Germany, erica.barkasz@dlr.de*

^f *Communications and Ground Stations, German Space Operations Center, German Aerospace Center (DLR), Reichenbergstrasse 8, 82362 Weilheim, Germany, amanuel.geda@dlr.de*

^g *Communications and Ground Stations, German Space Operations Center, German Aerospace Center (DLR), Reichenbergstrasse 8, 82362 Weilheim, Germany, christian.oetl@dlr.de*

* Corresponding Author

Abstract

Operations of deep space spacecraft depend strongly on the availability of respective communication assets. Large aperture antennas are available mainly in the hands of agencies such as NASA, ESA and JAXA, with a few more scattered in other agencies and commercial operators, however in terms of increasing requirements and needs the availability is scarce. The Weilheim 30m antenna has been constructed in the early '70s, that time for the joint NASA-DLR mission HELIOS. Since then it has been used less and less, until complete cease of operations. First with the advent of the Galileo program, a new need for precise signal measurement and validation was identified, which enabled a major mechanical overhaul in 2008. An increasing interest in large aperture reflectors over the last years brought the 30m antenna in Weilheim back to the focus. With this increasing interest DLR decided to upgrade the antenna, with the aim of being able to fully support deep space missions in the near future. Therefore, the antenna must be modified to achieve the best possible antenna performance in X-band while maintaining the L-band capability for in-orbit testing. Searching for best outcome with available resources, we came up with herein presented concept. Starting point of our considerations was is finite-elements and hybrid simulations, which were not possible in that extent some years ago and are still pushing the simulation tools to the limit. Apart from the technical antenna upgrade, there is a number of aspects which will need to be addressed in parallel. Starting from the antenna booking procedures, definition and implementation of antenna configuration in the operational phase, up to the integration inside the multi-mission environment and the newly introduced automation system. Additionally, the integration of the antenna in international networks and partnerships will pose significant effort but also open new possibilities for the community, giving favourable deep space communication capacity.

Keywords: DeepSpace, ground station, antenna, X-band, L-band, cross support, communications

Acronyms/Abbreviations

High Power Amplifier (HPA), Deutsches Zentrum für Luft- und Raumfahrt (DLR), Deep Space Network (DSN), Carbon Fiber Reinforced Polymers (CFRP), Antenna Control Unit (ACU), Low Noise Amplifier (LNA), Finite Elements Method (FEM), Equivalent Isotropic Radiated Power (EIRP), Antenna Gain to System Noise Temperature (G/T), In Orbit Test (IOT), In Orbit Verification (IOV)

1. Introduction

Deep space missions are characterised by several factors which influence many aspects of the overall mission design. Detailed planning of mission events, spanning many years is essential, as is the selection of the appropriate launch vehicles and the design of the spacecraft itself, which is expected to survive in a hostile environment for decades. In contrast to other mission types (e.g. LEO, GEO), the communication aspect plays a central role in deep space missions and is also given appropriate attention in the popular media [1].

The greatest challenge in communicating with such spacecrafts is without a doubt overcoming the vast distances and still be able to transmit and receive the required amount of data [27]. Distances of millions of kilometers are typical, and it's actually easier to talk about signal run-time than distance, which gives people a better sense of this. Deep space typically starts with the distance to spacecraft at the Moon and beyond, resulting in a round trip time of about 2.56 seconds [25] to several hours, as in the case of Voyager [2, 26].

One factor is time and another is the power flux density of the signal at the receiving end. This is very low in most cases. Large EIRP values can be achieved by combining high power amplifiers (which require significant input power) with high gain antennas. Neither can be transported by spacecraft or maintained in space. Therefore, the only way to overcome this issue is to use large ground-based facilities.

This leads us to the most important feature of deep space antennas - their size. The largest antennas used for spacecraft communications today are the DSN ones of 70 m diameter, located at Goldstone, Canberra and Madrid [3]. There are yet larger facilities such as Effelsberg [4], however mainly dedicated to radio astronomy and therefore do not have the needed communication capabilities, especially the uplink.

DLR's Ground station in Weilheim has been initiated in 1969, with the construction starting in 1967 [24]. The first satellite to be operated was the German mission AZUR in 1969 [5]. It took few more years, until the 30m antenna was built in Weilheim, intended to support a US American - German mission HELIOS [6]. The antenna system has been constructed in 1973 and went into operation in 1974 using S-band. Initially it was used as commanding station, whereas the reception of telemetry was performed by the radio telescope in Effelsberg. The mission has been supported until 1986, and in meanwhile the system was further extended by a receive path. Further the station supported the HELIOS 2 and Voyager missions. In 1982 the antenna has been upgraded to receive X-band signals. Other supported missions were Giotto [7] and Galileo [8] in 1989.



Fig. 1. Deep Space 30m Antenna in Weilheim, Designation S68

In the 1990s and early 2000s, the 30m antenna S68 was used only sporadically, even its decommissioning was discussed. Luckily, demolition of such a big metal construction was very expensive, thus these ideas were discarded. In 2008 the support of yet another Galileo spacecraft started, this time with validation and calibration measurements

for a new European navigation satellite positioning constellation. As there was a new use case for the antenna, in 2010 it got a major mechanical refurbishment.

Currently a space race to the Moon, to Lagrange points and into interplanetary space is in progress, involving not only well-known agencies, but also commercial providers and joint constellations. The number of missions planned, being in preparation, or already flying, which aim to explore space beyond Earth orbit, both robotically and astronautically, is impressive. In the meantime, apart from NASA and ESA, also the agencies and organisations from India [9], China [10], Israel [11], the United Arab Emirates [12] or South Korea [13] are striving towards the Moon or Mars with partly ambitious robotic missions. There are very concrete efforts to establish a lunar gateway [14], i.e. a space station in lunar orbit, from which astronauts are to carry out landings on the moon again in only a few years. Here, NASA is counting on an international collaboration similar to the ISS project.

All of these projects, which operate beyond Earth orbit, require Earth-based communications systems with appropriate transmitting power or correspondingly sensitive receiving characteristics. Thus, we decided begin a new project, aiming to expand the 30m antenna capabilities, so that it can be used for the deep space missions.

2. Current status

On the European level, only a single-digit number of comparable facilities exist, for instance as part of NASA's Deep Space Network (DSN) [15], ESA's ESTRACK system [17], or commercial operators [16].

The basic principle of this 30m antenna is still state of the art in satellite communications. It is designed as a near-field Cassegrain configuration [18]: As feeding antenna a Hoghorn is used. This gives the opportunity to install the receiver in-line with the elevation axis and independent of the current elevation angle during operations. For transmission, the Hoghorn deflects the energy from the horizontal direction to a perpendicular oriented aperture through a cut-out into the primary reflector. The wave front travels from this aperture to the subreflector, located in a near field distance from the Hoghorn. From there the wave is reflected to the primary reflector. Both reflectors are specially shaped for proper amplitude taper and possesses no dedicated focal point. The surfaces are designed to generate a plane wave front emanating from the primary reflector. This antenna structure is reciprocal, identical for transmit and receive mode of operation [Fig 2].

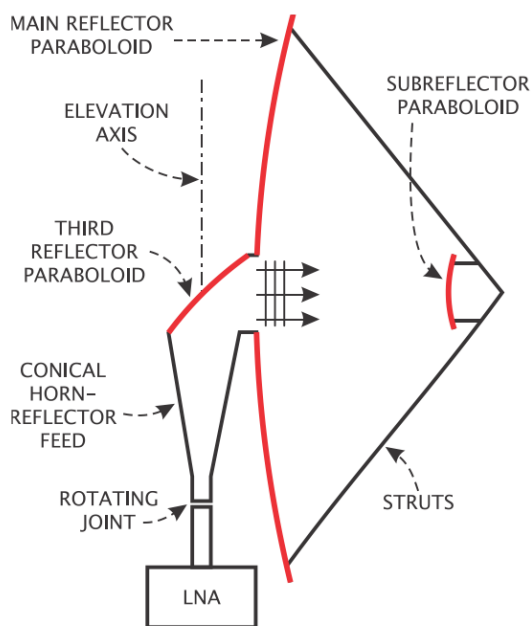


Fig. 2. Idealized sketch of the Near Field Cassegrain configuration

Currently the antenna is used for IOT/IOV support in L-band and to support deep space missions in X-band where possible with a limited X-band G/T of only about 44 dB/K. The lack of receiver sensitivity is due to the specially shaped antenna surface resulting from the original S-band use. Because of this geometry disadvantage for today's

usage, the entire effective antenna area is comparable to an antenna with a diameter in the region of 20m. More detailed information about the shape and how to remedy its disadvantage can be found in chapter 4.

For dual circular (RHCP / LHCP) signal reception in both frequency bands, a dual receive band feed system, developed and manufactured by MIRAD microwave, has been installed in 2017. In case of L-band usage, two fully independent measurement systems are in use to perform the payload in orbit testing. The first system is operated maintained and developed by the DLR institute of communication and navigation [29], the second test system was installed in 2018 by SES together with SED-systems on behalf of Spaceopal, as a backup for ESA's main IOT-system facility at the Redu ground station in Belgium [28]. Both systems are fully decoupled, and all calibrations and measurements have been conducted by different RF-specialists. This unique constellation of two completely independent measurement systems using the same antenna, allows to re-measure and verify suspicious results without changing the location. However simultaneous use is not possible, to fully avoid interference between the systems.

The antenna has no transmission capability at all at the moment. The original S-band transmit path, to send telecommands to a spacecraft had been removed during overhaul work in 2010 since then there was no use for it anymore.

At a first phase the potential of installing cryogenic low noise amplifiers was discussed and evaluated. There is no doubt that it would increase the Rx-sensitivity, but just installing new receivers has two major drawbacks:

1. The antenna gain won't be improved. Therefore, reaching the desired EIRP values needed for real deep space support would not be possible
2. The system noise temperature T_{Sys} of an antenna is composed of the antenna noise temperature T_A and the equivalent noise temperature of the receiver T_R . By installing a cryogenic LNA, T_R will be reduced (in our case about 30 Kelvin). But if T_A is significantly greater (e.g. due to a bad efficiency) than the temperature of the receiver, the improvement remains behind the expectations.

This gets clear by some simple calculations (example values)

Initial assumptions: T_A : 80 K, T_{R1} (normal LNA): 40 K T_{R2} (LNA with lower noise temperature): 10K, G (antenna gain): 60 dBi (remains a constant value in this example)

Table 1. Example calculations for G/T improvement

$T_S [K]$	$G/T_S [dB/K]$	Improvement to initial config [dB]	config
$80 + 40 = 120$	39.2	–	Initial config
$80 + 10 = 90$	40.5	1.3	New receiver
$40 + 40 = 80$	41.0	1.8	Lowered T_A
$40 + 10 = 50$	43.0	3.8	Lowered T_A plus new receiver

It can be seen that the improvement by just changing the LNA is in the range of the geometry update, and also that the overall result in this example can be improved significantly by doing both upgrades. In the current configuration, the antenna has a higher noise temperature, due to the increased sidelobe-levels and therefore noise pickup. It has to be noted also, that in this case the system noise temperature will decrease and the antenna gain itself will be increased, therefore the G/T – ratio becomes even greater.

Before starting the simulations, some RF measurements were performed for comparison and cross-checking with the later simulation results. Several antenna pattern cuts have been recorded via satellite and boresight, at satellite beacon frequencies, plus start- mid- and stop-frequencies. The L-/X-band feed system position was changed in order to make sure it won't affect the results. Therefore, also the HPBW (Half Power Beam Width) of the pattern cuts and the received power magnitude variation were observed.

The measurements have been performed inside the elevation cabin and were done with the original setup, using a 450mm long circular waveguide adapter and also by changing the position of the feed in between this range. The example picture below shows a 450mm long waveguide adapter followed by the L-/X-band feed. Next to it is a spectrum analyzer plot that shows a zero span (therefore the x-axis represents time domain) measurement performed tracking the XTAR-EUR beacon signal. During this 500 sec. long sweep, the position of the feed system has been changed and the distances for maximum and minimum values have been noted.

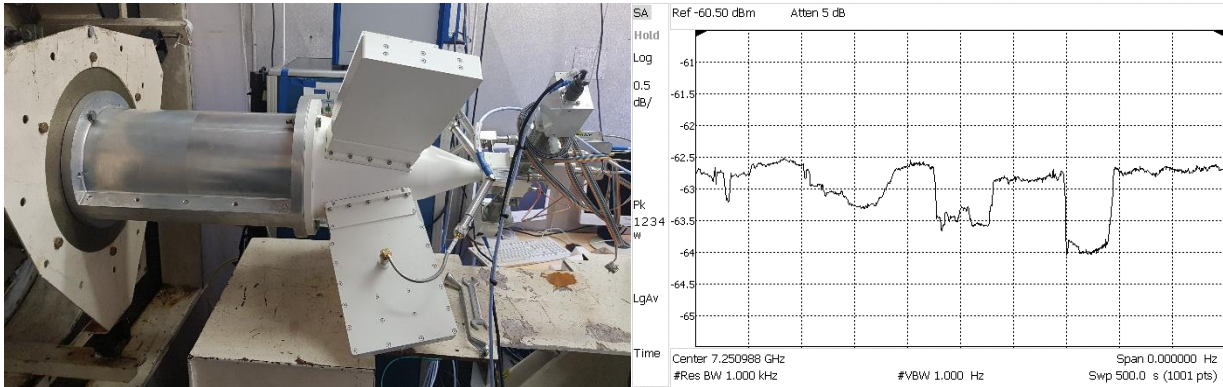


Fig. 3. left: 450mm adapter plus feed; right: zero span plot received power while shifting the feed position

After evaluation of the test results it was clear, that the original feed position fits best and there is no need to adapt the position. This is well aligned with the later simulation results.

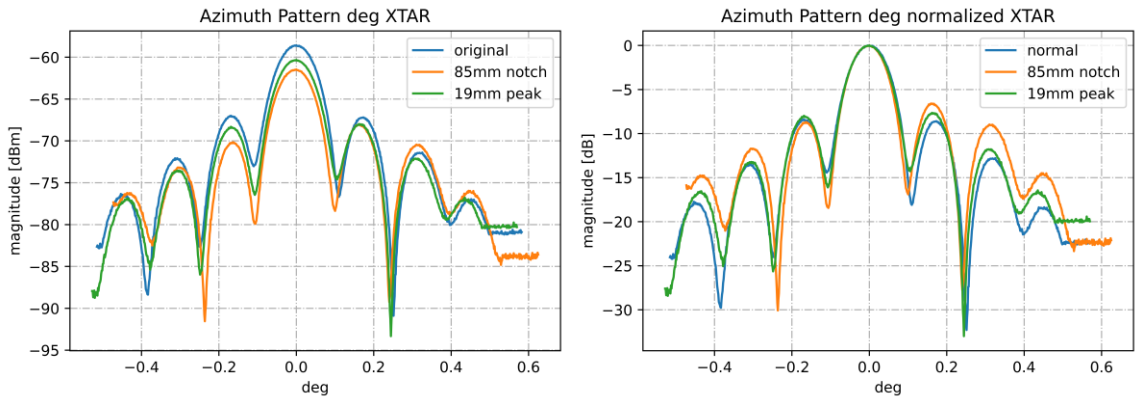


Fig. 4. left: azimuth pattern cut absolute values; right: azimuth pattern cut normalized power

The figure above shows three azimuth pattern cuts. “original” is the feed system directly mounted to the hog-horn flange, “85mm notch” was the position of the minimum Rx-power value at a distance of 85 mm away from the flange, and 19mm peak is the relative maximum that was found at a distance of 19mm distance from the flange. The feed system could not be moved with too much accuracy. Nevertheless, the measurements showed that a change of the feed position has no noticeable influence on the HPBW of the antenna and the focusing of the energy.

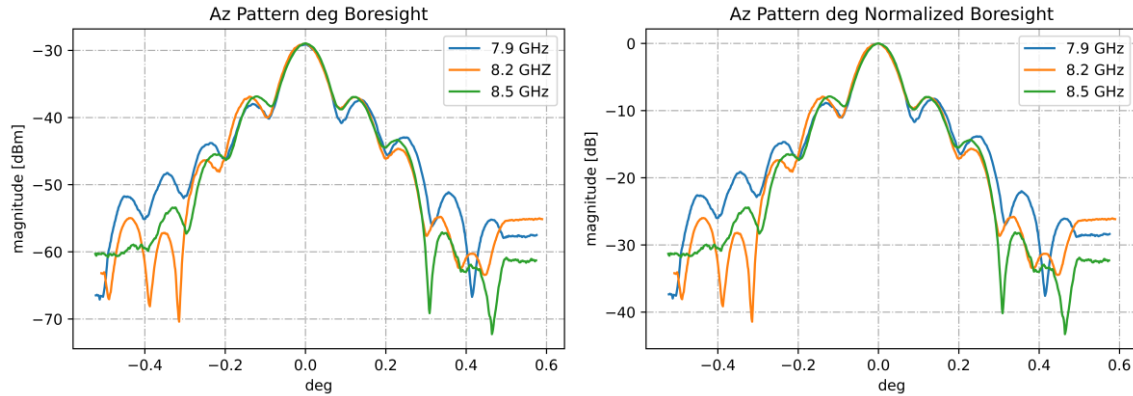


Fig. 5. Azimuth pattern cuts, via boresight measured at start- mid- and stop-frequency. Left: absolute; right normalized magnitude

The figure above shows three different pattern cuts measured at start- mid- and stop-frequency using the boresight facility. For all cuts the HPBW values have been calculated as well. Those were in good agreement with the first estimation by the rule of thumb formula: $\theta_{-3dB} = 70 \lambda/D$ (λ : wavelength; D : main reflector diameter)

Table 2. Measurement results for HPBW

frequency [GHz]	$\theta_{-3dB} meas$ [deg]	$\theta_{-3dB} calc$ [deg]
7.9	0.089	0.089
8.2	0.088	0.085
8.5	0.085	0.082

All measurements were done in both X- and L-band.

During the first simulations differences in antenna gain estimations in L-band between the measured data and the simulations occurred. By further investigation, a difference of about 20mm for the distance between the inferior end of the main reflector and the apex of the sub reflector was identified. After correcting the distance, there was a good agreement between the simulation and measured values.

With the installation of a cryogenic receiver also the need for electrical power and maintenance would increase significantly, without any improvement for the Tx-path of the antenna. Space missions to the moon or deep space missions in particular will always require corresponding transmission capability at least in the X-band. This is necessary to be able to send commands to a space probe at great distances. Weighing the arguments for and against a cooled receiver ultimately led to no longer pursuing this option in the first place.

The antenna is designed for deep-space missions in terms of servo drive system and positioning accuracy. The parameters of the antenna are shown in the following table.

Table 3. Current S68 antenna characteristics

Parameter	Value
Receive-Frequency [GHz] and Polarization	L-Rx 1.100 – 1.720 Dual circular (RHCP/LHCP) X-Rx 7.900 – 8.500 Dual circular (RHCP/LHCP)
Gain [dBi] @ [GHz] / (Efficiency)	48.9 @ 1.4 (40%) referred to LNA input 63.6 @ 8.42 (33%) referred to LNA input
G/T [dB/K] @ Elevation [°]	26.5 @ 5 (L-band) 44 @ 5 (X-band)
AZ/EL Speed [°/s]	1.5 / 1.0
Pointing Accuracy [deg]	±0.001

The following figure shows the Rx setup installed in L- and X-band as it is today. The received L-band signal can be routed to the two fully independent in-orbit verification measurement systems via a coaxial switch (L-Band Switching in block diagram). The measurement systems allow a quality analysis of the radiated Galileo signals.

In X-band, the received signal is converted to an intermediate frequency of 70 MHz via a downconverter and further fed to a baseband system (CORTEX) via a switch matrix. The baseband system then generates the telemetry data stream which is displayed in the control room.

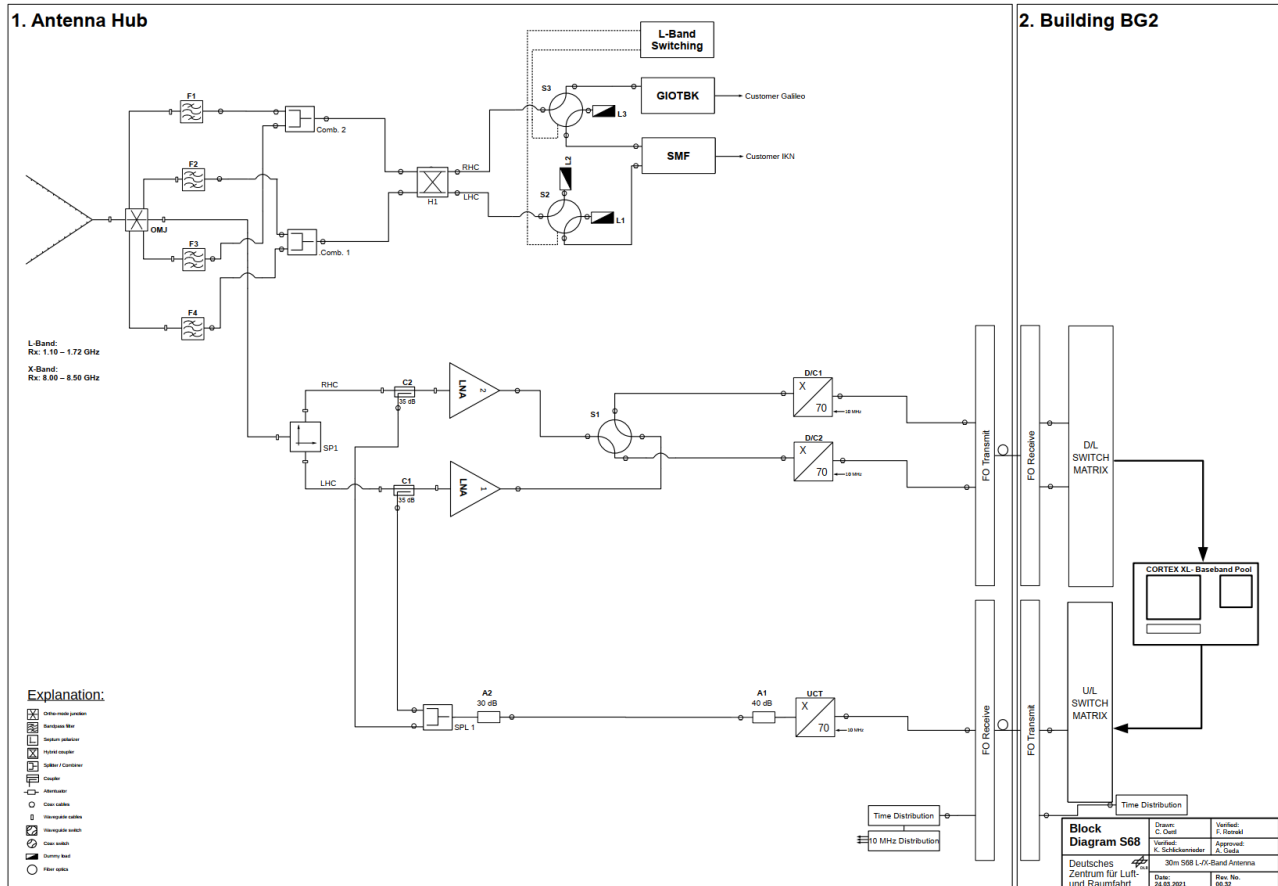


Fig. 6. Block diagram of the current reception path of the antenna

3. Identification of upgrade elements

The project involves mainly technical upgrades to the transmission and reception paths of the antenna, as well as significant changes in the main antenna section.

As indicated above, an improvement in antenna reception can be achieved by increasing the overall antenna efficiency and therefore the antenna effective area. This is achieved by recalculating the convex subreflector, remanufacturing it accordingly, and thus to achieve a better illumination of the main reflector. The above-mentioned improvement of the subreflector and the associated increase in the effective antenna diameter somewhere close to 30m already directly improves the transmission characteristics of the antenna as well.

Within the scope of this project, the antenna is to be upgraded to transmit in X-band. The output power of the high power amplifier shall be around 5 kW, which meets the EIRP requirements for sending commands to all mission

profiles we are expecting. An appropriate feed system has to be developed and produced. Reception shall be possible still in L- and X-band, as it is, plus the feed must be able to handle this huge amount of Tx-power, and still not affect the downlink. At the same time, the electrical connections and the power distribution system are to be renewed in order to comply with the current standards and laws in this respect. A major benefit with exchanging the sub reflector is that the antenna gain will be increased in both L- and X-band. So even the L-band IOT measurement systems will profit from the upgrade.

The signal processing of TT&C will be performed with Cortex CRT eXplorer, a product of Safran. This baseband unit is an upgrade of the current Cortex CRT XL. The operating intermediate frequency is 70 MHz in both forward link and return link. The Cortex CRT eXplorer supports the current error correcting codes as recommended by CCSDS: Turbo Codes and LDPC codes with all the rates as recommended [19]. It also supports the concatenated Convolutional and RS channel codes as recommended by CCSDS. It is good to remember that the concatenated code of the Convolutional code rate $\frac{1}{2}$ and the RS block code (255, 223) is in use since Voyager, 1977. The CRT eXplorer IF receiver could lock to IF signal as low as -120 dBm. If both RHC and LHC signals are received, the diversity combiner can be activated to maximize the SNR at the output of the combiner (maximum Gain of 3 dB is possible when both RHC and LHC signals are equal). CCSDS PN ranging will be supported in addition to the current ranging used in the station. The ranging unit, RAU, could support the ESA-Code, ESA-like, ESA Standard tone range, with tone frequency from 2 Hz up to 1.5 MHz; a distance measurement resolution of 1 ns. The phase noise of CRT eXplorer: -70 dBm/Hz at 10 Hz offset and -120 dBm/Hz at 1 MHz. A carrier sweep range up to 1000 kHz and a sweep rate from 1 Hz/s up to 175 kHz/s. It supports most of the suppressed carrier modulation in return link as recommended by CCSDS [21]: BPSK, QPSK, OQPSK, SOQPSK, GMSK, AQPSK [21]. It also supports the residual carrier modulation for deep space, BP-L/PM, as recommended [21].

The diagram on Fig. 7 shows the intended setup after the upgrade. The reception path stays largely unchanged, and a transmit path will be added. IF-signals will also be at a mid-frequency of 70 MHz. Transmission polarization will be dual circular (RHCP / LHCP) like the downlink and switchable hot-redundant, in case one of the upconverters will fail. The SSPA is intended to be solid state with internal redundancy. This means it consists of several stages that will be combined at the HPA output. In case one of the amplifier stages fails, the amplifier shall compensate for this failure as well as possible. Exchanging amplifier stages should be possible during operation. Power consumption is expected to be much less than with klystron or TWT systems, since the SSPA does not need to be operated permanently, has no long warm-up times and can be switched off completely if not used for some time where no passes are scheduled. The output can be switched do a dummy-load for testing purposes and diplexers will be needed together with the feed system to sperate Tx- and Rx- frequencies properly and prevent crosstalk. As indicated in the block diagram, the antenna will get the necessary connections in order to perform RF-compatibility tests (RFCT) after the upgrade. At the Weilheim Ground Station a RFCT facility (shielded room including a clean room tent) is available for S-band, and also a shielded cabin for Ku-band inside the antenna basement. Tests were also successfully completed in Ka-band. It is intended to integrate the X-band connections directly inside the main RFCT facility. Mainly all of the needed equipment for the transmit path upgrade must be procured through a tender process.

interfering signals be received by the antenna. In the first construction data the sub reflector was placed fully inside the main dish, not visible above the main aperture.

The current status of all reflecting surfaces were laser scanned by the Institute of Geodesy at the Universität der Bundeswehr (UniBwM) in 2010. The measured point cloud of the two reflectors is referred to axially symmetrical surfaces corresponding to polynomials of grade 6 and 8. Inside the Hoghorn an additional parabolic sector was scanned.

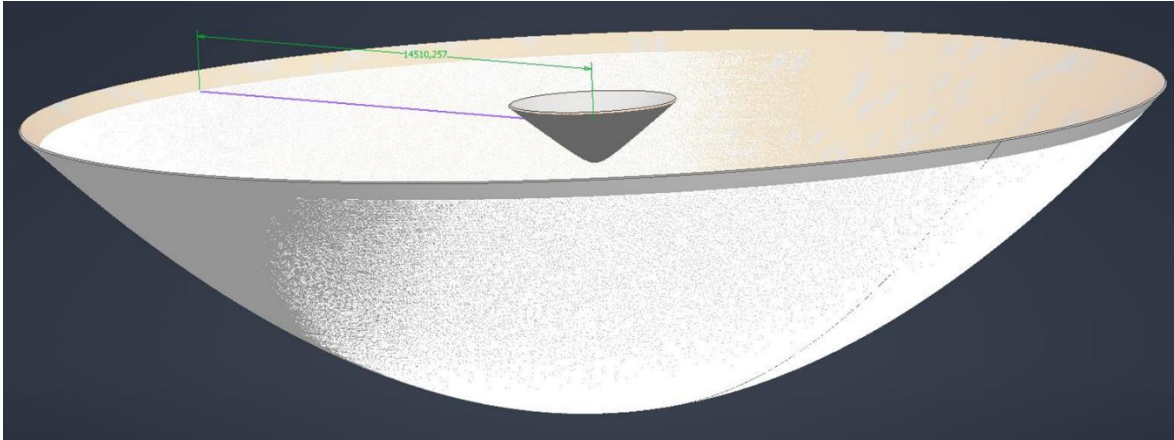


Fig. 8. Visualization of the scanned reflector surfaces

Thus, all surfaces can be modelled in a proper way in the EM-software ‘Electronics-Desktop’ (EDT) of ANSYS. This software provides a number of different solvers from full 3D ‘Finite Element Method’ (FEM), Integral Equation (IE) solver and Physical Optics (PO) in different implementations up to ‘Shooting and Bouncing Rays’ (SBR+).

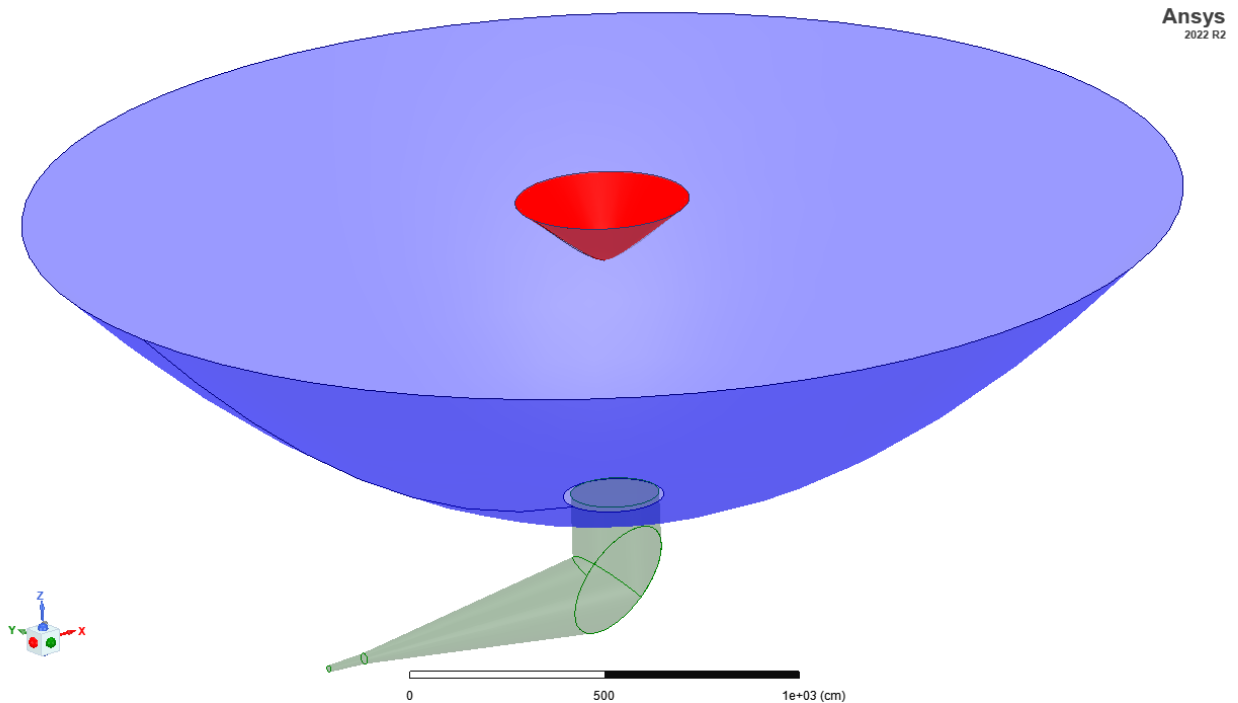


Fig. 9. ANSYS EDT 2022 R2 simulation model for optimizing the shaped reflector surface of the sub reflector (red). In blue the main reflector and the Hoghorn in green.

To validate the antenna model simulations at L- and S-band frequencies were performed and compared to real antenna gain measurements. The results are very promising and a more detailed investigation of the antenna system

could be started in the EM-software. It could be shown that the safety margin in the main reflector reduces the antenna gain considerably as well as an additional failure in phase at the aperture. As a result, structural elements of the antenna system have to be modified to optimize the antenna for higher gain.

Most of the structural elements are frequency independent and meet the rules of physical optics very well. An optimization at lower frequencies might have a positive outcome also in the X-band area. Due to the near field character this is only true for the reflectors, not for the Hoghorn feed. The Hoghorn is a complex structure, appearing like a 90-degree bended conical horn. Inside the bend a parabolic section, with focal point at the beginning of the conical horn, is installed. This conical horn cannot be treated as a frequency independent structure. At X-band the horn aperture is about 60 wave lengths wide. The focal length is about 9450mm.

The near field pattern of the Hoghorn is, at all frequencies, not symmetric. In longitudinal direction the maximum in amplitude and phase distribution is slightly shifted to the direction of the horn input. Due to the parabolic section the polarization purity of the horn is reduced. We are looking only for operations with circular polarization. without any symmetrical plane the horn has to be modelled in its full extend. At L- and S-band this is not an issue for a 3D FEM simulation. But at X-band it appears to be rather challenging. We perform our calculations on a Windows Server infrastructure with 1.5TB RAM memory. This configuration shows up to be too weak as the full 3D simulation demands more than 9TB RAM. Together with ANSYS we optimize the Hoghorn model to be solved at X-band frequencies. The EDT provides hybrid simulation techniques with a joint FEM-IE boundary condition. Excessive use of that feature helps to reduce the mesh volume to a minimum. The horn now can be calculated in less than one week of time on 1.3TB RAM.

With the help of this 3D model, the field distributions are calculated via the finite element method in the various frequency bands. In the process, the gain of the antenna can also be determined. The next figure shows the field distributions in the critical areas.

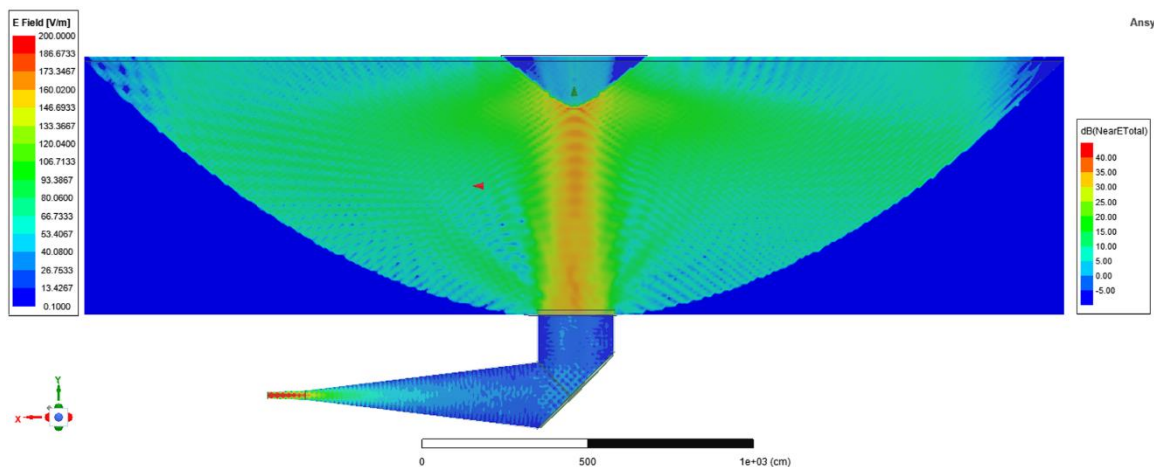


Fig. 10. Rendering of E-field distribution in Hoghorn and reflector areas. Hoghorn is linear scaled whereas the reflector area is logarithmic scaled to represent the field distribution at 1.15 GHz for proper visibility.

By changing the shape of the subreflector, the antenna gain in the main beam direction is now to be increased. The aim is to achieve an area efficiency of 70%.

With the increase of the antenna gain, the sensitivity (G/T) and radiated power (EIRP) to the receiving location will be increased. Analyses have shown that with an optimization of the reflector arrangement the illumination could be improved and thus a power increase of the antenna (gain) of approx. 2.4 dB maximum could be achieved. With the procurement of a 5kW amplifier (HPA) and an improvement of the antenna gain, an EIRP of around 100 dBW would be achieved. The receive path figure of merit G/T is expected to increase to a value of about 46.9 dB/K, so that all ESA requirements could be met. Both values are based on more pessimistic calculations for an overall efficiency around 50%. In case the update will increase the efficiency to 70% even higher numbers can be expected, see the table below.

Table 4. S68 antenna expected characteristics after upgrade

Parameter	Value (after upgrade)	Example ESA requirements
Frequency [GHz] and Polarization	L-RX 1.100 – 1.720 Dual circular (RHCP/LHCP) X-RX 7.900 – 8.500 Dual circular (RHCP/LHCP) X-TX 7.145 – 7.235 Dual circular (RHCP/LHCP)	L-RX 1.100 – 1.720 Dual circular (RHCP/LHCP) X-RX 7.900 – 8.500 Dual circular (RHCP/LHCP) X-TX 7.145 – 7.235 Dual circular (RHCP/LHCP)
Gain [dBi] @ [GHz] / (Efficiency)	51.3 @ 1.4 (70%) 55.6 @ 2.295 (70%) 66.9 @ 8.426 (70%)	N/A
TX-Power flange HPA	36 dBW	N/A
EIRP [dBW] (2dB loss)	100.9 dBW	Minimum 93 dBW (100 dBW for MEX)
G/T [dB/K] @ Elevation [°]	37.4 @ 5 (L-band) 47.4 (X-b and)	46 (X-band)
AZ/EL Speed [°/s]	1.5 / 1.0	1.0 / 1.0
Pointing Accuracy [deg]	±0.001	±0.005

5. Operational aspects and integration in Multi-Mission environment

One of the challenges in the whole project will be the operational integration of the antenna. Currently it is semi-integrated only, due to its limited use for few very specific missions. Semi-integration means, that the antenna control (like pointing, gears, etc.) is already implemented in our multi-mission station monitoring and control system, called WARP. Due to the special use, the scheduling and other operational tasks are not included in our daily automated processes. One could say, the 30m antenna in Weilheim is an outsider not only with respect to its size, but also operationally.

First aspect of an operational integration will be the integration in our new scheduling system (GSSNG, [22]) and definition of the antenna characteristics. We will have to adopt the antenna specifics like longer setup and reset times into the scheduling procedures. Our current approach is also to try to treat the antenna exactly the same like all others we have on site. Here it is worth to mention, that our Weilheim station is very specific, as it includes all different kinds of antennas – from small and medium sized antennas for LEO satellites, few antennas for GEO use (like IOT and TOSS), few for GEO as anchor stations, and finally the 30m deep space dish. Now the deep space seems to be kind of a combination of GEO antenna use (long contact times, services like ranging and Doppler) and LEO (antenna following the spacecraft track, yet slow). We need to analyse if such combination imposes any specific impact on a scheduling process. Aspects which may count are things like handling of the interruptions during a pass (caused for example by occultation) or the way of communicating configuration change (like EIRP, data rate). Also accounting of support time (by hours or other measure?) or communication with mission operations (are they always available?) will play a role.

We can shortly mention here the communications aspect. In principle it is expected, that the data rates which the antenna will provide for deep space missions will not be very high, thus current data link capacity (10Mbps) shall be enough. Special case may be imposed however by the high data rate Moon communications, where real-time links in X-band could reach easily several tenths or even up to hundred Mbps. And this possibly for very long periods of time. In such a case we will have to consider to either extend the existing bandwidth or procure additional lines independent on multi-mission context.

Integration into the multi-antenna monitoring and control system (called WARP) will be performed in parallel to the upgrade activities. As soon as manufacturers of each device deliver us documentation and specification of their equipment, the integrator team will start with implementing necessary plugins and interfaces. Finally, the automation of various processes and services within the system will be configured. Here we expect to have same or very similar automation as for our other antennas on site, potentially just fed with slightly different parameter values (like for example duration).

Operations with the antenna is intended to be as flexible as it is with the other antennas in the multi-mission area. In usual operations the customer books the antenna one week in advance (it can be extended up to three months), the passes are semi-automated (tests for full automations are currently running), online and offline product delivery is already automated, we offer on site operators 24x7 and engineering on call service.

Still, there are missions which require a different approach, as in the case of Akatsuki, the contacts are booked a year in advance since there are few and unique opportunities for the radio experiments, in this particular case incoming

and outgoing product are processed all offline by our Flight Dynamic Team and the contacts are performed by engineers. In the case of LEOPs (one of the few cases with higher priority) the booking is done around 2 weeks prior the launch and changes dynamically with the possible launch delays, all contacts are performed by engineers in permanent voice contact with the customer and all products incoming and outgoing are online (real time).

6. Summary and outlook

The 30m antenna at DLR's ground station in Weilheim is getting a significant upgrade, which will allow us to get back to real deep-space operations. We hope that the antenna will find its permanent place in international deep-space networks, and will provide useful services to the community and help pushing the boundaries of human exploration. Special focus on upcoming years will be dedicated to Moon missions, and for this the S68 antenna will be a perfect companion, allowing for very high data rates at these distances.

In the future we may reconsider further upgrading the S-band path, which will be largely dependent on future missions, if they will require this frequency band. As the current upgrade limits the feed to the X- and L-band only, and would not easy allow for respective tri-band replacement (L-, S- and X-band), other solution would need to be implemented, for example with a beam waveguide including multiple wave mirrors and thus allowing for switching between different feed systems without changing their coupling to the waveguide every time.

Further options which we may rather consider, would be provision of Delta DOR (DDOR) services, which will be possible with open-loop recording functionality of our new basebands. It will be needed to provide respective recording space as well as time reference and decide on the way of provision of such data. The DDOR service will impact actually several aspects of operations, for example usage of scheduling system with CCSDS Service Management DDOR Pattern formats. This option will therefore involve significant integration efforts.

Finally, to improve the reception sensitivity, we may decide to install cryogenic LNA's, which would increase the G/T even more. This could improve the antenna performance enough, to actually support high data rate Mars missions.

References

- [1] Movie "The Dish", <https://www.imdb.com/title/tt0205873/>, Accessed 24. January 2023.
- [2] Ludwig, Roger; Taylor, Jim (March 2002). "[Voyager Telecommunications](#)" (PDF). NASA. Retrieved 24 January 2023.
- [3] NASA / JPL DSN https://www.nasa.gov/directorates/heo/scan/services/networks/deep_space_network/about , Accessed 24. January 2023.
- [4] Max-Planck-Institut for Radioastronomy, <https://www.mpifr-bonn.mpg.de/en/effelsberg> , accessed 24. January 2023
- [5] 50 Jahre AZUR, https://www.dlr.de/content/de/artikel/news/2019/04/20191107_50-jahre-azur.html , accessed 26.01.2023
- [6] Helios 1 & 2 <https://honeysucklecreek.net/dss44/helios.html>, Accessed 24. January 2023.
- [7] Giotto, <https://solarsystem.nasa.gov/missions/giotto/in-depth/>, Accessed 24. January 2023.
- [8] Galileo, <https://www.jpl.nasa.gov/missions/galileo>, Accessed 24. January 2023.
- [7] Imbriale, William A. Large antennas of the deep space network. John Wiley & Sons, 2005.
- [9] Jitendra Nath Goswami, Mylswamy Annadurai, Chandrayaan-1 mission to the Moon, Acta Astronautica, Volume 63, Issues 11–12, 2008, Pages 1215-1220.
- [10] Ouyang Ziyuan et al., Chang'E-1 Lunar Mission: An Overview and Primary Science Results, Chin. J. Space Sci. (2010), Volume 30(5), Pages 392 ff

- [11] Gibney, Elizabeth. Israeli spacecraft Beresheet crashes into the Moon. *Nature* 568, no. 7752 (2019): 286.
- [12] Almaeeni, S., Els, S., and Almarzooqi, H.: The Rashid rover: to guide the way for the next generation lunar missions and solar system exploration, EGU General Assembly 2021
- [13] Ju, G., Bae, J., Choi, S., Lee, W.B., and Lee, C. J., New Korean Lunar Exploration Program (KLEP), An Introduction to the Objectives, Approach, Architecture and Analytical Results. 64th International Astronautical Congress, Beijing, China, 2013.
- [14] Sean Fullera et al., Gateway Program Status and Overview, 72nd International Astronautical Congress, Dubai, United Arabic Emirates, 2021
- [15] Imbriale, William A. Large antennas of the deep space network. John Wiley & Sons, 2005.
- [16] Gunhilly Ground Station <https://www.goonhilly.org/>, Accessed 24. January 2023.
- [17] E. Vassallo et al., "The European Space Agency's Deep-Space Antennas," in Proceedings of the IEEE, vol. 95, no. 11, pp. 2111-2131, Nov. 2007
- [18] Di Maria, A. et al. (2014) High Fidelity Modeling of 30m Near-Field Cassegrain Antenna in X-band. In: 8th European Conference on Antennas and Propagation (EuCAP). EuCAP 2014, 2014-04-06 - 2014-04-11, Den Haag, Niederlande.
- [19] CCSDS 131.0-B-4, TM Synchronization and Channel Coding, Blue Book, Washington, April 2022
- [20] Kenneth Andrews et al., The development of Turbo and LDPC codes for deep space applications, Proceedings of the IEEE Vol. 95, No. 11, November 2007
- [21] CCSDS 401.0-B-32, Radio Frequency and Modulation Systems—Part 1: Earth Stations and Spacecraft, Blue Book, Washington, October 2021
- [22] M. Gnat at al, Scheduling as an interoperability service and its security aspects, SpaceOps 2014, Pasadena, USA
- [23] https://www.dlr.de/content/de/artikel/news/2020/04/20201112_destiny-deutschland-und-japan-starten-asteroidenmission.html, Accessed 24. January 2023.
- [24] Kuss, P. et al, 50 Jahre Satellitenbodenstation Weilheim, DLR Raumflugbetrieb und Astronautentraining, Limited edition, 2017
- [25] The Moon, <https://www.dlr.de/content/en/articles/moon-special/the-moon.html> , accessed 26.01.2023
- [26] Voyager Telemetry Signal, https://voyager.jpl.nasa.gov/news/details.php?article_id=76 , accessed 26.01.2023
- [27] ESA and DLR in joint study to support deep space missions, https://www.esa.int/Enabling_Support/Operations/ESA_and_DLR_in_joint_study_to_support_deep_space_missions, accessed 26.01.2023
- [28] ESA IOT System, https://elib.dlr.de/63559/1/2009_IAIN_Stockholm_LatestDevelopmentsPLIOTOfGalileoIOVSpacecraft_published.pdf, accessed 27.01.2023
- [29] DLR IKN IOT System, <https://ieeexplore.ieee.org/stamp/stamp.jsp?tp=&arnumber=6423110>, accessed 27.01.2023